GeoHazards

MDPI

Article

GIS-Based Landslide Susceptibility Modelling in Urbanized Areas: A Case Study of the Tri-City Area of Poland

Anna Malka

Polish Geological Institute—National Research Institute, Branch of Marine Geology, 5 Kościerska St., 80-328 Gdansk, Poland; anna.malka@pgi.gov.pl

Abstract: This paper presents the results of landslide prediction modelling for young glacial areas performed using statistical methods. The area in question is urbanized and therefore mass wasting activity is a matter of interest to both the local community and the authorities. The analysis was based on the 2011 'Register of landslides and areas prone to mass movements with a scale of 1:10,000 for the city of Gdansk' and the 2012 incomplete 'Register of landslides and areas prone to mass movements with a scale of 1:10,000 for the city of Gdynia'. The research took into account geological, geomorphological, hydrological, hydrogeological, and anthropogenic conditions. The landslide susceptibility map was created using the statistical landslide index. The calculated indices were used to create a map of Gdansk's landslide susceptibility. In Gdansk, 84.50% of the total diagnosed landslide area belongs to the high susceptibility class, 14.25% to the moderate susceptibility class, and only 1.25% to the low or very low susceptibility class. After extrapolation, the data was also used to create a susceptibility map for the remaining parts of the Tri-City area, Sopot and Gdynia. The difficulty of extrapolating landslide data for neighboring urban areas was indicated. In Gdansk, which had been covered by geological mapping, the best modelling results were obtained with a large number of causal factors. In Gdynia and Sopot, for which the statistical landslide index value was extrapolated from Gdansk, the best results were obtained when selected causal factors were considered. In Sopot and Gdynia, 81.6% of the landslide area belongs to the high susceptibility class, 15.1% to the moderate class, and 3.3% to the low susceptibility class. These results emphasize a different role of some causal factor classes in the occurrence of landslides in neighboring urban areas. The resultant maps show the areas in which mass wasting is the most probable in the future.

Keywords: modelling; landslide susceptibility; landslide susceptibility index; morainic upland; Tri-City area of Poland

1. Introduction

Mass wasting processes, controlled by gravity, hydrologic response, and strong-ground motion conditions, are important geodynamic hazards that can significantly affect local economies. The damaging nature of landslides is particularly dangerous in densely populated urban areas. The Tri-City area of Gdansk, Gdynia, and Sopot is an example of such an area, located in a terrain with very diverse topography. The negative impacts of mass wasting may lead to enormous damage to property. In 2001 alone, after violent rains, damage caused by landslide activation in Gdansk was estimated at EUR 780,000 [1]. Currently, many landslides in Gdansk are still active, as confirmed by terrestrial laser scanning techniques monitoring of selected shallow landslides carried out in 2014–2022 [2]. However, awareness of these types of hazards in the Tri-City area is low, as comprehensive geological research on the area's landslides has been carried out only recently [1–7].

Risk management involves identifying the extent of risk, introducing appropriate preventative methods to mitigate the risk, and decreasing the possibility of the harmful incidence or minimizing the vulnerability or exposure to the risk factors [8]. One of the many methods of managing landslide risk, commonly used worldwide, is to determine

locations susceptible to mass wasting using geographical information systems (GIS) tools and statistical methods. During the last decades, the ever-growing availability of earth observation data and the well-established use of GIS has led to the development of automated workflows based on GIS toolboxes [9,10].

Landslide susceptibility maps are an instrument used to support land management. Landslide susceptibility assessment is a valuable tool for land use planning and reducing the costs of landslides [11,12]. Landslide susceptibility assessment can also be considered as an important tool in early warning system techniques, as well as the initial step towards the landslide hazard and risk assessment [13]. The literature provides many examples of GIS being harnessed in mass wasting research (e.g., References [14–18]). Many diverse techniques are used to study landslide susceptibility, including the empirical, statistical, and deterministic approach used in large-scale engineering geology projects [15,19].

In Poland, geoinformation analyses of landslides have been performed only since the early 2000s, mainly in the mountainous areas of southern Poland [20–23] and for the remaining part of Poland in the areas characterized by intensive human activity [6,7,24]. The importance of landslide susceptibility assessments for environmental policy and decision-making processes in Europe is set forth in the framework of the European Union's Thematic Strategy for Soil Protection [25]. The relevance of landslide zoning through spatial susceptibility assessments in Europe is additionally recognized in the European Commission's approach to natural and man-made disaster prevention [26]. Additionally, landslides are among the natural hazards that the European Union considers particularly important and had a high priority in the EU forest strategy for 2030 [27]. Therefore, many studies evaluate landslide susceptibility in the context of multi-hazard assessments [18].

This paper presents the results of shallow landslide prediction modelling in the urbanized Tri-City area of Poland using the statistical landslide index (SLI) method. The bivariate SLI method has been used by various researchers [6,7,17,18,28–31]. So far, however, whether the susceptibility indices developed by this method would be applicable in neighboring areas has not been validated. This article presents the results of the extrapolation and, in addition, a comparison of the two susceptibility maps for the cities of Gdansk [6] and Gdynia [32] produced using the SLI method. The article also compares the role of individual passive factors for these two neighboring areas.

This type of extrapolation of data for neighboring areas has not been discussed extensively in the literature. According to Smith et al. [33], spatial analysis is a process that in many instances follows a number of (often iterative) stages. Therefore, some researchers carry out multiple iterations of susceptibility modelling of the same area to improve prediction performance and comparison [34,35].

The primary source of information is the 2011 'Register of landslides and areas prone to mass movements with a scale of 1:10,000 for the city of Gdansk'. In all, 96 landslides were identified in Gdansk at that time. They account for 0.12% of the city's area (Jurys et al., 2014) [1]. The results of the landslide inventory in Gdansk were then extrapolated to the neighboring cities Gdynia and Sopot. The extrapolation results were verified by landslides occurring in 2012 for selected areas of Gdynia. Extrapolation for Gdynia and Sopot was carried out in 2013, but the results have not been published so far. In 2015, a complete landslide inventory was prepared for Gdynia [5], which was then updated as part of the author's doctoral thesis [32]. On the basis of this research, susceptibility maps were produced for Gdynia [7,32].

2. Location and General Features of the Study Area

The Tri-City consists of three metropolitan centres: Gdansk, Gdynia, and Sopot. The area is greatly diversified in terms of its geomorphology and geology (Figure 1).
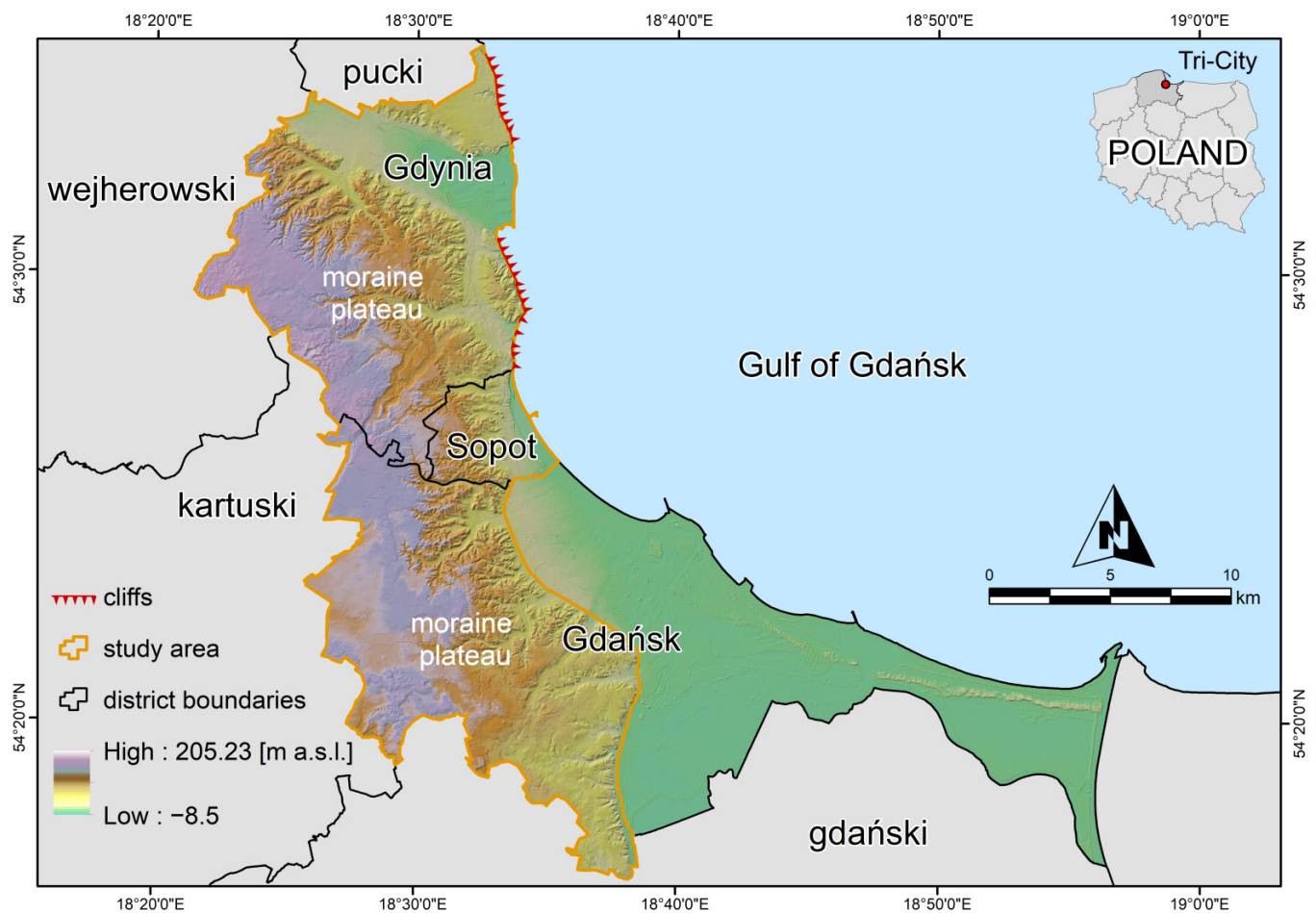
Figure 1. Location of the study area. District boundaries are administrative boundaries. District is the second-level unit of local government and administration in Poland.

The local climate is influenced by elevation and the distance from the Baltic Sea. The altitude ranges from −8.5 to 205.23 m above sea level. The very location of the Tri-City, characterized by the hypsometric diversity of the terrain surface, affects the high variability of atmospheric precipitation. According to the Polish Climate Atlas, normal precipitation in the time period between 1971 and 2000 ranged from about 550 mm in the area of the coastal zone to about 700 mm in the eastern part of the moraine plateau of the Kashubian Lakeland [36]. The mean annual maximum air temperature observed in the period between 1951 and 1998 was 11 °C [37].

As late as the 19th century, buildings in Gdansk and Sopot were located on flat coastal and river areas [38–40]. In the Tri-City, for the last few decades, the slopes of uplands and the slopes of valleys have also been included in the development [1]. In the Tri-City between 1997 and 2016 the greatest changes took place in arable land, which altogether decreased by 17%, and forest land (13% in total). All this was to the benefit of grassland (which increased by 23%) and built-up areas (increasing by 10% in total) [41]. The land cover change caused an increase in the landslide occurrence, causing more severe property damage [32].

In terms of geomorphology, the study area is mainly located within the moraine plateau (Figure 1). It was formed during the Weichselian glaciation as a result of the accumulation of moraine deposits, i.e., tills, sands, and gravels. During deglaciation, the moraine plateau was incised by a glacio-marginal outflow system [42]. The edges of the moraine plateau were cut by erosional valleys [43]. The Tri-City's western upland, located within the boundaries of the peripheral part of the Kashubian Lakeland which developed in the Pleistocene, is the most prone to landslides. Furthermore, also threatened by landslides are the slopes of the Kashubian Coast upland, covering the eastern part of Sopot and Gdynia, along with a relatively small north-western part of Gdansk [44]. The eastern boundary of the Kashubian Coast comes in direct contact with the Gulf of Gdansk to create a cliff shoreline, which is the most susceptible to landslides of all of the Tri-City areas (Figure 2a–d).
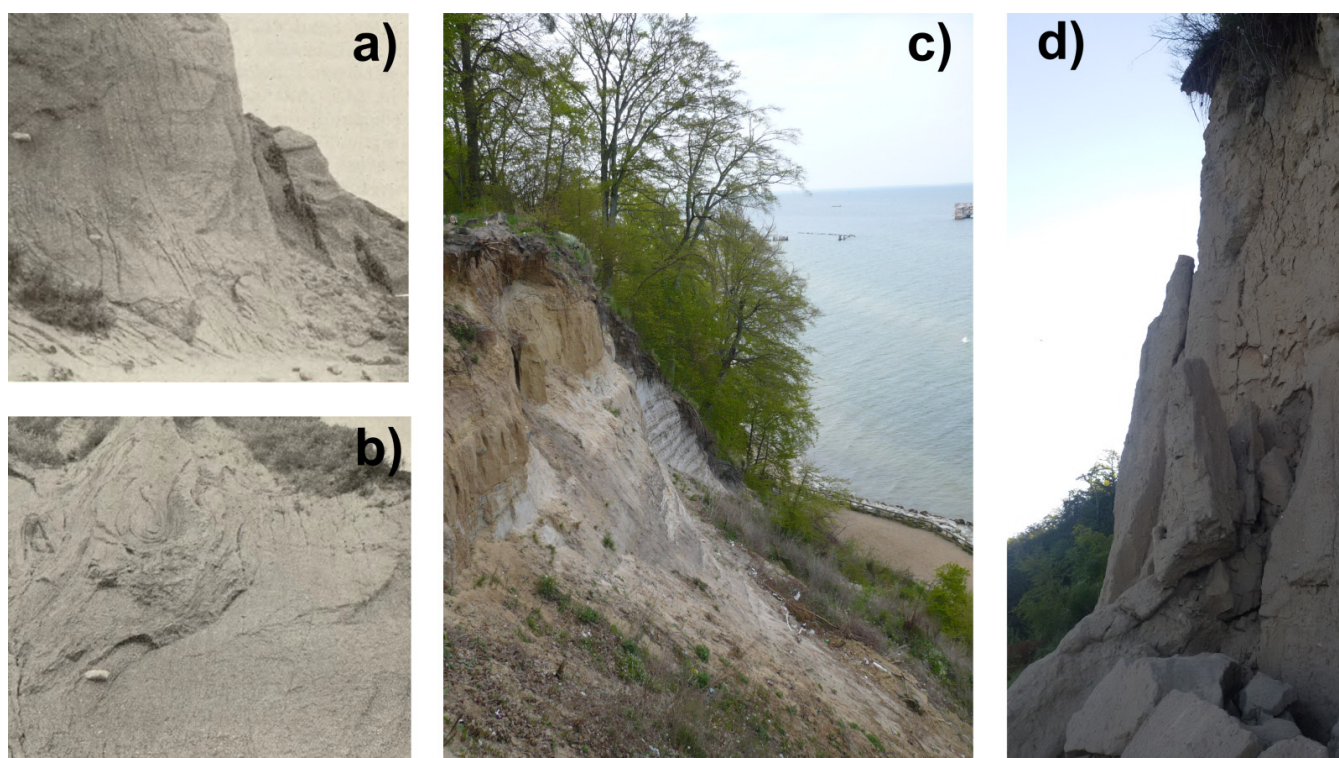

Figure 2. (**a**) Earth fall developed in glacial till at Oksywie Cliff [45]; (**b**) earth slide at Oksywie Cliff, escarpment carved in Pleistocene glacitectonic sands and silts [45]; (**c**) earth slide in Babie Doły, Gdynia, escarpment carved in Pleistocene glacial till and Neogene glaciotectonic rafts inside glacial till, May 2012 (photo: Małka); (**d**) earth fall developed in glacial till at Redłowo Cliff, August 2016 (photo: Małka).

The mass wasting which occurs there is initiated and aggravated by abrasion. The cliffs began to form approximately 6000 years ago and their general shape remains similar to this day [46,47]. The earliest information on threats related to mass movements in the area of present-day Gdynia dates from the end of the 16th century and relates to cliff coasts (Małka 2019) [48]. The first geological survey for these cliffs was carried out in the early 20th century (Figure 2a,b) [45].

At present, the development of Baltic cliff shorelines is the most influenced by the eustatic factor, with its activity regionally modified by the neotectonic factor with minimal influence from glacial isostatic movements [49]. In the Tri-City area, negative (subsiding) vertical movements of the Earth crust surface were detected at a value of (−1.1) mm/year, to additionally increase the relative growth of sea level in the area [50].

From a geological point of view, the Tri-City area features Quaternary formations of significant thickness, reaching as much as 145 m [51], with Neogene lacustrine formations locally exposed in situ and in the form of glacial float [45,51–53]. For the most part, the Tri-City area is covered by sandy-gravelly fluvioglacial sediments and tills of the morainic upland, with silty-clayey marginal lake sediments occurring in places [54]. The lowered terrain is filled with diverse Holocene sedimentary facies [52,53]. In the Tri-City's urbanized sections, a clear relationship can be observed between the geological structure and its resultant land morphology and the occurrence of shallow landslides. Pronounced drops in terrain, varied slope angles, and the conducive geological structure produce good conditions for landslides. The presence of non-homogenous glacial, marginal lakes and fluvioglacial sediments, as well as multiple glaciotectonic deformations, is highly significant. Moreover, an important role is played by formations with aleurite grain size, which are prone to being washed away and liquefied. They are exposed at the fringe of the Kashubian Lakeland's morainic upland [1].

Land development methods and human activity important factors initiating the occurrence and development of shallow landslides in the Tri-City. Many present-day landslides originated from anthropogenic changes in land use. Undercutting, over-steeping of slopes, and construction burden, coupled with faulty water and sewage management, have an especially negative influence [1]. The problem of landslides occurring in the urbanized areas of the Tri-City has been known since the second half of the 20th century and is still ongoing, causing significant damage to infrastructure (Figure 3a–d).

Figure 3. (**a**) Earth slide in Biskupia Górka, Gdansk (http://kronikarp.pl, 1981 (accessed on 16 May 2016)); (**b**,**c**) earth slide and earthflow in Karwiny, Gdansk March 2022 (photograph by Małka and Maciaszek); (**d**) damage road caused by landslide in Kamienna Góra, Gdynia February 2017 (photograph by Jurys).

3. Input Data

The research material for landslide susceptibility maps of the Tri-City area was provided by Poland's National Geodetic and Cartographic Resource, with additional source data from the Polish Geological Institute, National Research Institute, and public domain materials (Table 1). The following data have been used for the purpose of the GIS analysis: the digital elevation model (DEM) from airborne laser scanning (ALS), also described as light detection and ranging data (LIDAR data) [55] from the Information System of Country Protection Against Extraordinary Hazards (ISOK) project; the Polish Topographic object database (BDOT database); maps of sediment type at a depth of 1 and 4 m b.g.l. from the 'Geological and engineering atlas of the Tri-City of Gdansk-Sopot-Gdynia Urban Area' [54]; a map of the groundwater table level; the Urban Atlas database [56]; the 'Register of landslides and areas prone to mass movements with a scale of 1:10,000 for the city of Gdansk' [3]; and the 'Register of landslides and areas prone to mass movements with a scale of 1:10,000 for the city of Gdynia' [4].

Table 1. Spatial digital data used in GIS analysis.

Digital Data	Source	Websites
Landslide inventory	Polish Geological Institute, National Research Institute (Jurys et al., 2011, 2012) [3,4]	https://geologia.pgi.gov.pl (accessed on 23 August 2022)
Digital elevation model	National Geodetic and Cartographic Resources	https://www.gov.pl/web/gugik (accessed on 23 August 2022)
Topographic object database	National Geodetic and Cartographic Resources	https://www.gov.pl/web/gugik (accessed on 23 August 2022)
Digital engineering geological data	Polish Geological Institute, National Research Institute (Frankowski et al., 2007) [54]	https://geologia.pgi.gov.pl (accessed on 23 August 2022)
Urban atlas	European Environment Agency (60. Urban Atlas–PL006L–Gdansk 2010) [56]	https://land.copernicus.eu/local/urban-atlas (accessed on 23 August 2022)

The accuracy of the layers used in the analysis corresponds to the cartometric accuracy of a 1:10,000 map. The resolution of all the raster maps used in the analysis is 5 × 5 m.

Thematic layers were collected, sorted, and prepared to showcase the causal factors. The research considered geological, geomorphological, hydrological, hydrogeological, and anthropogenic conditions. Selected causal factors visualized in the form of maps were used to model the landslide susceptibility of Gdansk and Gdynia (Table 2) [6,7].

Table 2. Explanatory variables used in SLI analysis and their influence on shallow landslide development.

No	Variable	Data Source	Influence on Shallow Landslide Mechanisms
1	slope angle (S)	DEM	Slope angle controls the balance of resisting and destabilizing forces acting on a slope [57].
2	slope aspect (A)	DEM	Slope aspect has an influence on solar radiation intensity, which controls the local temperature and evaporation [58]. The slope aspect also affects soil moisture, rainfall intensity, and vegetation density on the hillsides [29].

Table 2. *Cont.*

No	Variable	Data Source	Influence on Shallow Landslide Mechanisms
3	topographic wetness index (TWI)	DEM	TWI describes the influence of topography on the spatial distribution and extent of saturation areas [59].
4	stream power index (SPI)	DEM	SPI is a measure of the erosive force of water runoff [60].
5	the sediment transport capacity index (LS)	DEM	The LS index stands for sediment transport capacity, predicts the location of erosion, and shows the spatial distribution of potential soil losses [59].
6	relief energy (R)	DEM	Relief describes the gradients of the terrain and controls mass movements [6,7]
7	land use and land cover (LULC)	Urban atlas	LULC is associated with urbanization processes. Urbanization results in permanent changes to the landscape, the spread of an urban environment, and an increase in anthropogenic activities [61].
8	distance from watercourses and reservoirs (DWR)	Topographic object database	River erosion and sea abrasion as well as drainage density determine the likelihood of a landslide in young morainic areas [6,7]. Close river proximity induces instability at the foot of a slope due to the concentration of groundwater flow; further, river and sea undercutting also have a destabilizing effect [19].
9	ground type at a depth of 1 m b.g.l. (G 1)	Digital engineering geological data	Influence on the weathering of the bedrock and the resulting soils [62]
10	ground type at a depth of 4 m b.g.l. (G 4)	Digital engineering geological data	Deep geological structure has an impact on landslides in young glacial areas as it illustrates changes in permeability of sediments and potential slip zones [7].
11	groundwater table level (GW)	Digital engineering geological data	Well-sorted, fine-grained deposits in which the groundwater table is within 3 m may be subject to possible severe liquefaction [63].
12	elevation (E) *	DEM	Elevation relates to landslides trigger, i.e., heavy rainfall [7]
13	profile curvature (P) *	DEM	Divergent or convergent curvature has an influence on the water run-off concentration [64]

* Factor used only in landslide susceptibility mapping of Gdynia.

The selection of geospatial data for the Tri-City area was determined by relevance, reliability, and compatibility of scales. Although the Tri-City has a substantial amount of geospatial data, many of these sources (e.g., detailed geological maps of Poland, geoengineering data) were rejected in the analysis as they did not meet the above-mentioned criteria.

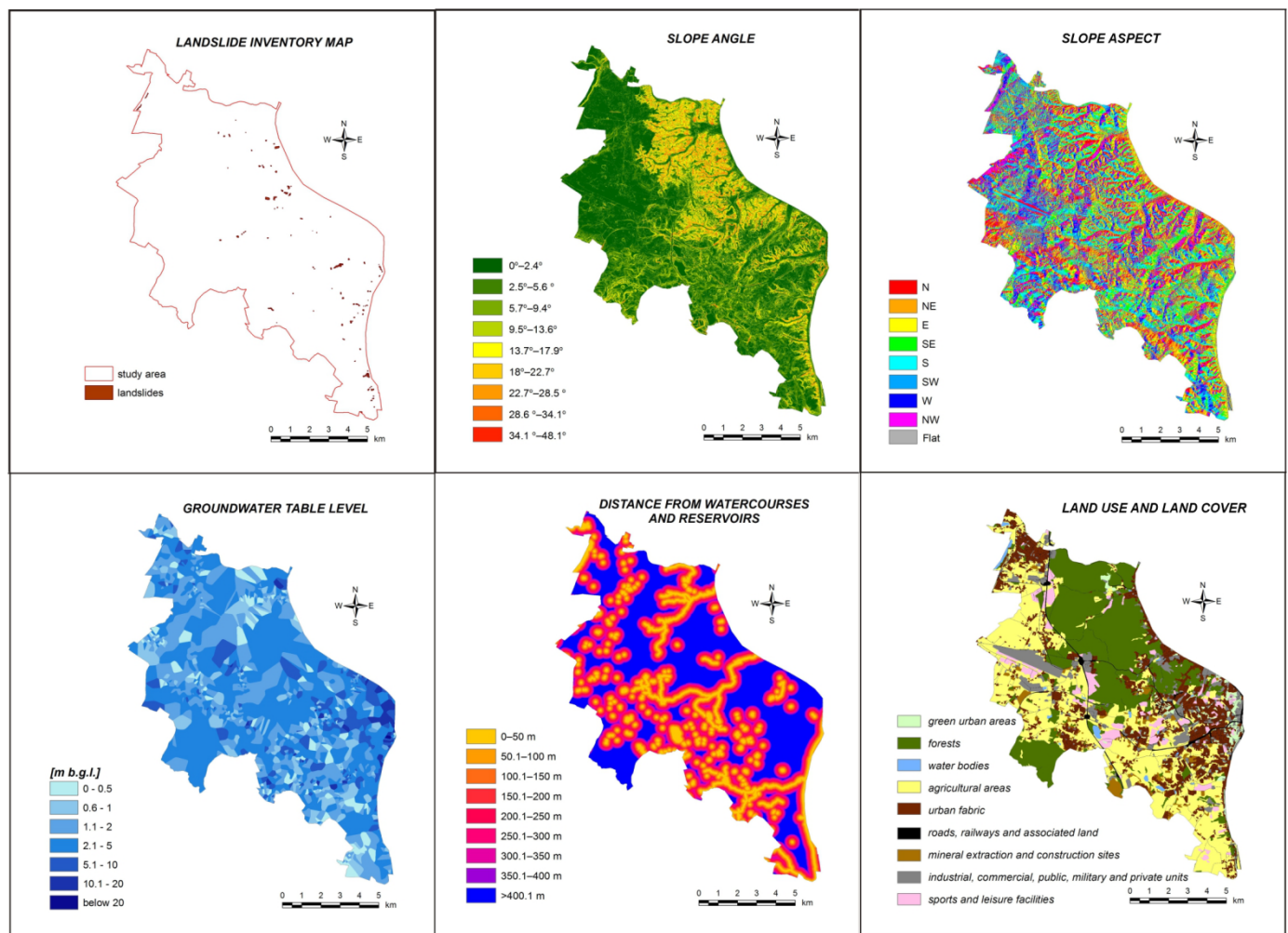The five selected factors are shown in Figure 4.

Figure 4. Selected thematic layers used in the GIS analysis in the Gdansk area.

4. Research Methodology

The landslide inventory was carried out with a scale of 1:10,000, in the framework of the LCS (SOPO) project, using standardized methods (Grabowski et al., 2008) [65]. The 'Register of landslides and areas prone to mass movements with a scale of 1:10,000 for the city of Gdansk' [3] was the basic source of information for the analysis and data validation of the susceptibility map of Gdansk.

The analysis considered the western part of the city of Gdansk, as the eastern part is flat and not affected by landslides (Figure 1). As Gdansk only has a small number of active landslides, all the landslides (96) were included to achieve reliable geoinformation analysis using statistical methods. For susceptibility modelling, the entire landslide area (landslide body) was considered.

Due to the already-performed comprehensive geological charting of Gdansk area landslides [1,3], a statistical analysis was performed for this area first. The set of inventoried landslides in Gdansk was divided into two spatially diversified subsets of 66 and 30 [6]. The larger subset and parameter maps were used to develop the model, while the second subset was used to verify it [6]. In modelling the landslide susceptibility of the area under research, 11 causal factors visualized as maps were used (Table 2) [6]. The topographic attributes, computed directly from the digital elevation model, included the slope angle, slope aspect, relief (computed in the preset vicinity of 5 m from each raster cell), topographic wetness index (TWI), stream power index (SPI), and the LS sediment transport capacity index. The primary and secondary topographic attributes were calculated directly from the high-resolution DEM obtained by airborne laser scanning (ALS) from 2014. The point

density in the ALS-based point cloud was 12 points/m². The Jenks natural break algorithm was used for grouping slope angles, elevation, relief energy, TWI, SPI, and LS [6,66–68]. The remaining parameter layers include: land use and land cover, distance from watercourses and reservoirs, maps of ground type at a depth of 1 and 4 m b.g.l., and the groundwater table level, computed on the basis of borehole data from geological and engineering documentation by means of Euclidean allocation (Table 2) [6].

The data obtained during field work (MOTZ map) and the maps which visualize the environmental factors were used to calculate the landslide susceptibility indexes by means of the landslide susceptibility [14,17,31]. The statistical landslide index (SLI) method used in the analysis is based on the following formula:

$$\ln W_i = \ln \left(\frac{Densclas}{Densmap} \right) = \ln \left(\frac{\frac{Npix(Si)}{Npix(Ni)}}{\frac{\sum Npix(Si)}{\sum Npix(Ni)}} \right)$$

ln W_i —the weight (landslide susceptibility index) given to a certain parameter class;
Densclas—the landslide density within the parameter class;
Densmap—the landslide density within the entire map;
Npix(Si)—the number of pixels which contain landslides in a certain parameter class;
Npix(Ni)—the total number of pixels in a certain parameter class.

The main premise of this method is the 'crossing' of a landslide map with a certain parameter map. The calculated landslide susceptibility indexes were used to create a landslide susceptibility map of Gdansk with a scale of 1:10,000 [6].

After extrapolation, the data was also used to create a susceptibility map with a scale of 1:10,000 for Sopot and Gdynia, the remaining areas of the Tri-City. To assign the SLI values to individual classes the intervals were selected by the Jenks (1967) [66] natural break algorithm. Determined in this way, the intervals made it possible to obtain the model's optimum predictive capacity, while at the same time narrowing down the susceptible areas, which is of great significance to the Tri-City.

The susceptibility map produced for Sopot and Gdynia was validated with the incomplete 'Register of landslides and areas prone to mass movements with a scale of 1:10,000 for the city of Gdynia' [4].

The article also compares the results of the susceptibility assessment for Gdansk and Gdynia, performed using the same methods for the entire landslide area. Comparison of the two susceptibility maps for neighboring urbanized areas was performed on the basis of the landslide susceptibility map of Gdansk, developed using the landslide susceptibility index (LSI) and eleven parameters (Table 2) [6], and the landslide susceptibility map of Gdynia was created using LSI and thirteen parameters (Table 2) [32].

The calculated weights (*ln W_i*) allowed the graphical representation of the role of the individual causal factors. The graphs were developed using Microsoft Excel 2010; for the sake of readability, the description of the individual factor classes was omitted in the graphs.

The spatial analysis of the landslide susceptibility maps of the Tri-City was performed using ArcGIS 10.2 software (https://www.esri.com (accessed on 23 August 2022)). Global Mapper 14.2 software (https://www.bluemarblegeo.com (accessed on 23 August 2022)) was used in an auxiliary capacity for data conversion and to change the resolution of the DEM data.

5. Results

Landslide susceptibility is determined by considering the interplay between landslide occurrences and impacts of factors that induce instability [7]. In this analysis, the use of the statistical landslide index and eleven thematic layers has revealed the importance of many environmental factors. Various combinations of instability factors were used in the modelling. Figure 5 presents the landslide susceptibility map of Gdansk with a scale of 1:10,000 developed using the SLI method, eleven variables, and all landslides.
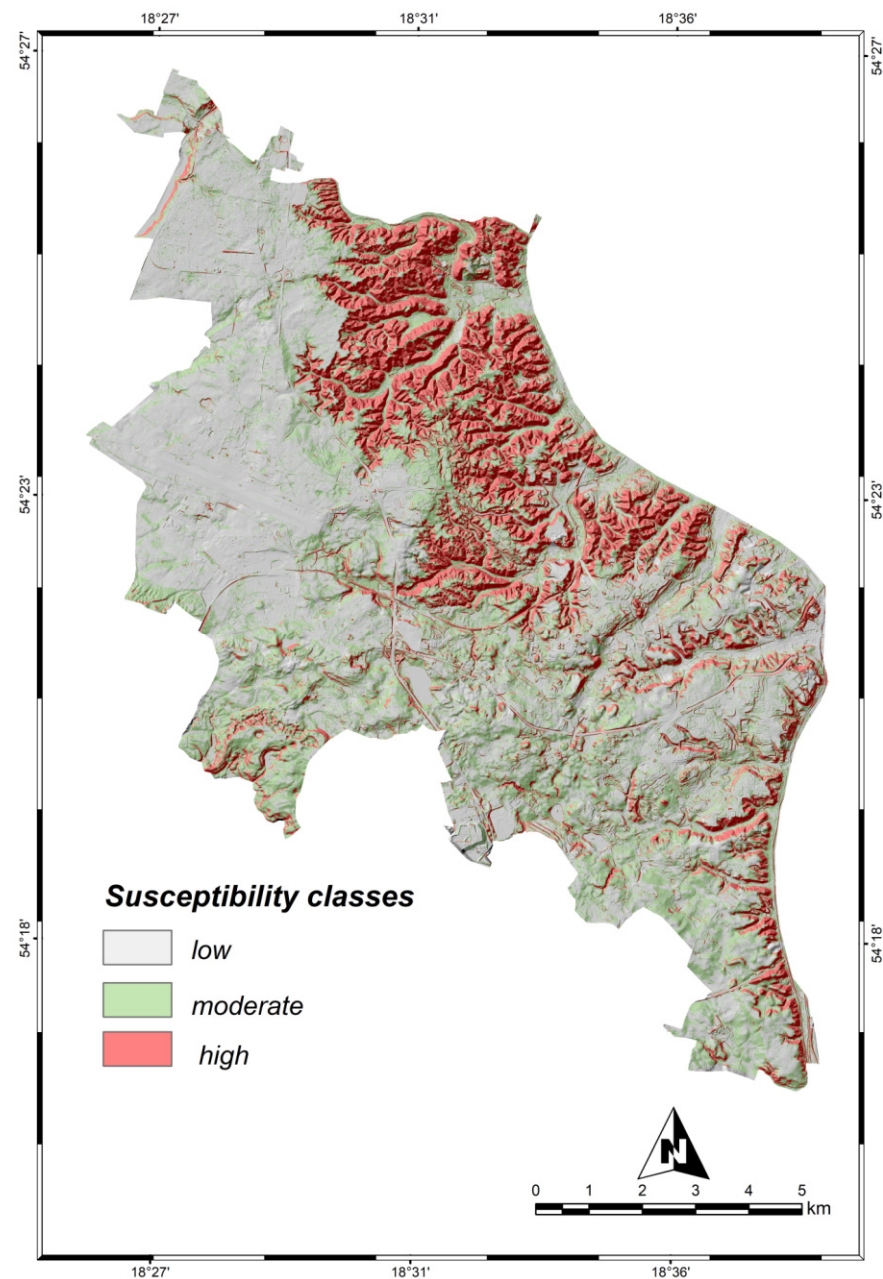
Figure 5. Landslide susceptibility map of Gdansk developed using statistical landslide index (SLI).

In the next stage, the LSI index in Gdansk was used to create a landslide susceptibility map for the neighboring counties of Sopot and Gdynia, which have a similar geological structure and equivalent geomorphological conditions. Not all the layers computed for the Gdansk area were applicable to the rest of the Tri-City. The limitation was the different scopes of the relief map and the LS sediment transport capacity index map for Gdansk and the rest of the Tri-City. For this reason, these data were not included in the secondary analysis. Greater slope angle values were found in the area of Sopot and Gdynia (from 0 to 63.4°) compared to Gdansk (from 0 to 48.1°). However, there was a growing dependence between the values of the lnWi index and the slope angle in Gdansk (Table 3), which is why the slope angle was applicable in the predictive model.

Table 3. Spatial relationship between the selected important conditioning factors and all landslides using the SLI for the entire landslide area in Gdynia and Gdansk. The LSI values (lnWi) were calculated on the basis of the updated landslide inventory for Gdynia from 2018 [32] and for Gdansk on the basis of the complete landslide inventory from 2011 [3]; values with different signs (plus/minus) are highlighted in yellow.

			Gdynia						Gdansk		
Causal Factor	Class	Ln W_i	Percentage of Landslide Pixels [a]	Percentage of Class Pixels [b]	Frequency Ratio (a/b)	Causal Factor	Class	Ln W_i	Percentage of Landslide Pixels [a]	Percentage of Class Pixels [b]	Frequency Ratio (a/b)
		[–]	[%]	[%]	[–]			[–]	[%]	[%]	[–]
Slope angle [°]	0–3	−3.57	1.34	47.67	0.03	Slope angle [°]	0–2.4°	−3.94	0.74	37.29	0.02
	3–8	−1.03	7.36	20.66	0.36		2.5–5.6°	−2.10	3.18	25.84	0.12
	8–14	0.29	18.80	14.11	1.33		5.7–9.4°	−0.42	8.67	13.20	0.66
	14–19	0.80	19.99	8.96	2.23		9.5–13.6°	0.72	16.57	8.04	2.06
	19–23	1.08	14.50	4.93	2.94		13.7–17.9°	1.22	20.49	6.04	3.39
	23–28	1.52	12.67	2.77	4.58		18–22.7°	1.38	20.25	5.10	3.97
	28–34	2.72	9.82	0.65	15.22		22.7–28.5°	1.65	18.06	3.48	5.19
	34–41	4.06	11.55	0.20	58.18		28.6–34.1°	2.32	8.21	0.80	10.20
	41–63	4.36	3.97	0.05	78.60		34.1–48.1°	2.99	3.83	0.19	20.03
Slope aspect	NW	−0.19	9.05	10.99	0.82	Slope aspect	NW	0.40	16.17	10.86	1.49
	W	−0.11	7.98	8.94	0.89		W	−0.82	4.44	10.09	0.44
	S	−0.20	9.44	11.54	0.82		S	−0.19	10.83	13.08	0.83
	SE	−0.23	10.83	13.63	0.79		SE	−0.40	9.01	13.41	0.67
	SW	−0.28	6.91	9.15	0.76		SW	−0.33	7.72	10.74	0.72
	E	0.49	23.72	14.58	1.63		E	−0.10	12.59	13.87	0.91
	N	−0.17	12.58	14.94	0.84		N	0.43	21.30	13.85	1.54
	NE	0.18	19.48	16.23	1.20		NE	0.24	17.90	14.09	1.27
	flat	−8.88	0.00	0.00	0.00		flat	−7.84	0.00	0.00	0.00
Distance from watercourses and reservoirs [m]	0–50	1.37	25.57	6.51	3.93	Distance from watercourses and reservoirs [m]	0–50 m	0.84	19.69	8.49	2.32
	50–100	0.63	12.86	6.86	1.87		50.1–100 m	0.69	17.04	8.57	1.99
	100–150	−0.67	3.65	7.17	0.51		100.1–150 m	0.13	10.46	9.20	1.14
	150–200	−0.85	3.14	7.35	0.43		150.1–200 m	−0.59	5.15	9.32	0.55
	200–250	−0.45	4.61	7.25	0.64		200.1–250 m	−0.91	3.61	9.00	0.40
	250–300	−0.02	6.79	6.93	0.98		250.1–300 m	−0.23	6.57	8.30	0.79
	300–350	0.34	9.15	6.52	1.40		300.1–350 m	−0.57	4.32	7.59	0.57
	350–400	0.03	6.30	6.11	1.03		350.1–400 m	−0.82	2.93	6.65	0.44
	>400	−0.49	27.74	45.23	0.61		>400.1 m	−0.08	30.19	32.89	0.92
Groundwater table level [m]	0–0.5	0.88	14.53	6.02	2.41	Groundwater table level [m]	0–0.5 m	−0.62	3.06	5.64	0.54
	0.5–1	0.27	32.58	24.94	1.31		0.5–1 m	−0.87	3.83	9.15	0.42
	1–2	−0.40	5.75	8.54	0.67		1–2 m	0.24	34.88	27.38	1.27
	2–5	−0.28	40.14	53.11	0.76		2–5	−0.21	38.95	48.22	0.81
	5–10	0.21	6.95	5.65	1.23		5–10 m	0.59	14.66	8.11	1.81
	10–20	−3.68	0.04	1.48	0.03		10–20 m	1.14	4.63	1.47	3.14
	below 20	−8.88	0.00	0.25	0.00		below 20 m	−7.84	0.00	0.03	0.00

Table 3. *Cont.*

Causal Factor	Class	Ln W_i	Percentage of Landslide Pixels [a]	Percentage of Class Pixels [b]	Frequency Ratio (a/b)	Causal Factor	Class	Ln W_i	Percentage of Landslide Pixels [a]	Percentage of Class Pixels [b]	Frequency Ratio (a/b)
		[–]	[%]	[%]	[–]			[–]	[%]	[%]	[–]
Land use and land cover	industrial and military units	−3.51	0.29	9.54	0.03	Land use and land cover	industrial and military units	−1.85	1.23	7.89	0.16
	urban fabric	−1.20	4.69	15.58	0.30		urban fabric	−0.47	9.66	15.42	0.63
	roads, railways and associated land	−3.10	0.27	6.03	0.05		roads, railways and associated land	−2.22	0.46	4.32	0.11
	mineral extraction and construction sites	−5.40	0.00	0.59	0.00		mineral extraction and construction sites	−3.01	0.15	2.97	0.05
	green urban areas	1.88	9.22	1.41	6.55		green urban areas	0.55	2.96	1.72	1.72
	sports and leisure facilities	−4.27	0.04	2.86	0.01		sports and leisure facilities	−2.91	0.25	4.67	0.05
	agricultural areas	−2.95	0.67	12.85	0.05		agricultural areas	−0.21	26.30	32.56	0.81
	forests	0.13	57.41	50.16	1.14		forests	0.68	58.92	29.78	1.98
	water bodies	−8.88	0.00	0.03	0.00		water bodies	−7.84	0.00	0.71	0.00
	coastal zone	3.46	27.39	0.86	31.98						

At the next stage, similar causal factor maps as for Gdansk were developed for the remaining part of the Tri-City (Gdynia and Sopot). Computed for the area of Gdansk by means of the SLI method, the landslide susceptibility indexes (lnWi) were then extrapolated onto the areas of Sopot and Gdynia. As a result of multiple iterations, a number of landslide susceptibility models were produced with the use of various parameter layers.

Five parameter layers were used in the final modelling of landslide susceptibility in Sopot and Gdynia: slope angle, slope aspect, land use, distance from watercourses and reservoirs, and the groundwater table level (Figure 6). The other parameter layers were not included in analysis, as they did not enhance the model's predictive capacity.

As a result, a landslide susceptibility map with a scale of 1:10,000 was produced for Sopot and Gdynia. Figure 7 presents the landslide susceptibility map of Sopot and Gdynia with a scale of 1:10,000, developed using the SLI method and five variables.

Based on the statistical analysis, a spatial layout of landslide-susceptible areas in the Tri-City was produced. The landslide susceptibility maps were verified in the case of Gdansk by means of the second landslide subset [6] and in in the case of Gdynia by means of the landslides documented during the incomplete 2012 cartographic field work for selected areas of Gdynia. Consequently, it was found that 84.50% of the landslide area diagnosed in Gdansk belongs to the high susceptibility class, 14.25% to the moderate susceptibility class, and only 1.25% to the low or very low susceptibility class [6]. High and

very high landslide susceptibility classes are found mainly in the north-east (the districts of Oliwa, VII Dwór, Brętowo, Wrzeszcz Górny) and in the east (Orunia-Św. Wojciech-Lipce) of Gdansk (Figure 5).
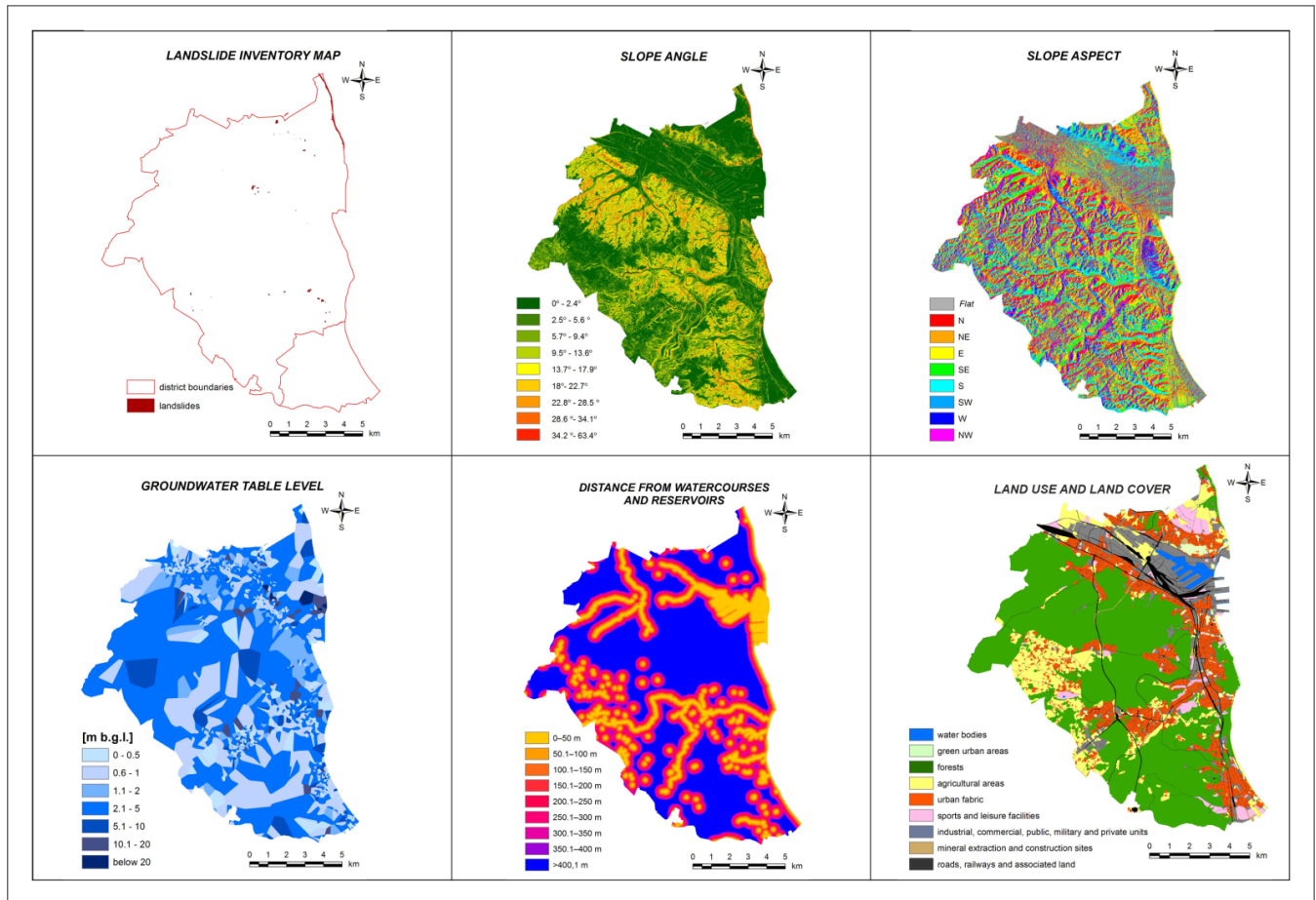

Figure 6. Thematic layers used in the GIS analysis in the areas of Gdynia and Sopot.

In Sopot and Gdynia, 81.6% of the landslide area belongs to the high susceptibility class, 15.1% to the moderate class, and 3.3% to the low susceptibility class. High landslide susceptibility is related to the cliff in the Oksywie and Redłowo Hillocks (Kępa Oksywska, Kępa Redłowska) and the area of the Tri-City Landscape Park.

Comparison of the two susceptibility maps for neighboring urbanized areas was performed on the basis of the author's previous research [6,7,32]. The application of the SLI method and many variables (11 for Gdansk and 13 for Gdynia) allowed for the determination of the importance of predisposing factors for Gdansk and Gdynia (Table 2) [6,7,32].

In the modelling of the landslide susceptibility of Gdansk using the SLI method and many causal factors, the most significant geo-environmental variables were the topographic attributes such as slope angle, relief energy, and LS; noteworthy also were TWI and SPI (Figure 8). Similar causal factors had the greatest impact on landslide formation in Gdynia (Figure 9) [7,32]. Furthermore, analogous classes had an impact on landslide formation in both cities. However, there was some differences in the individual classes of these factors for the two cities (Figures 8 and 9; Table 2).
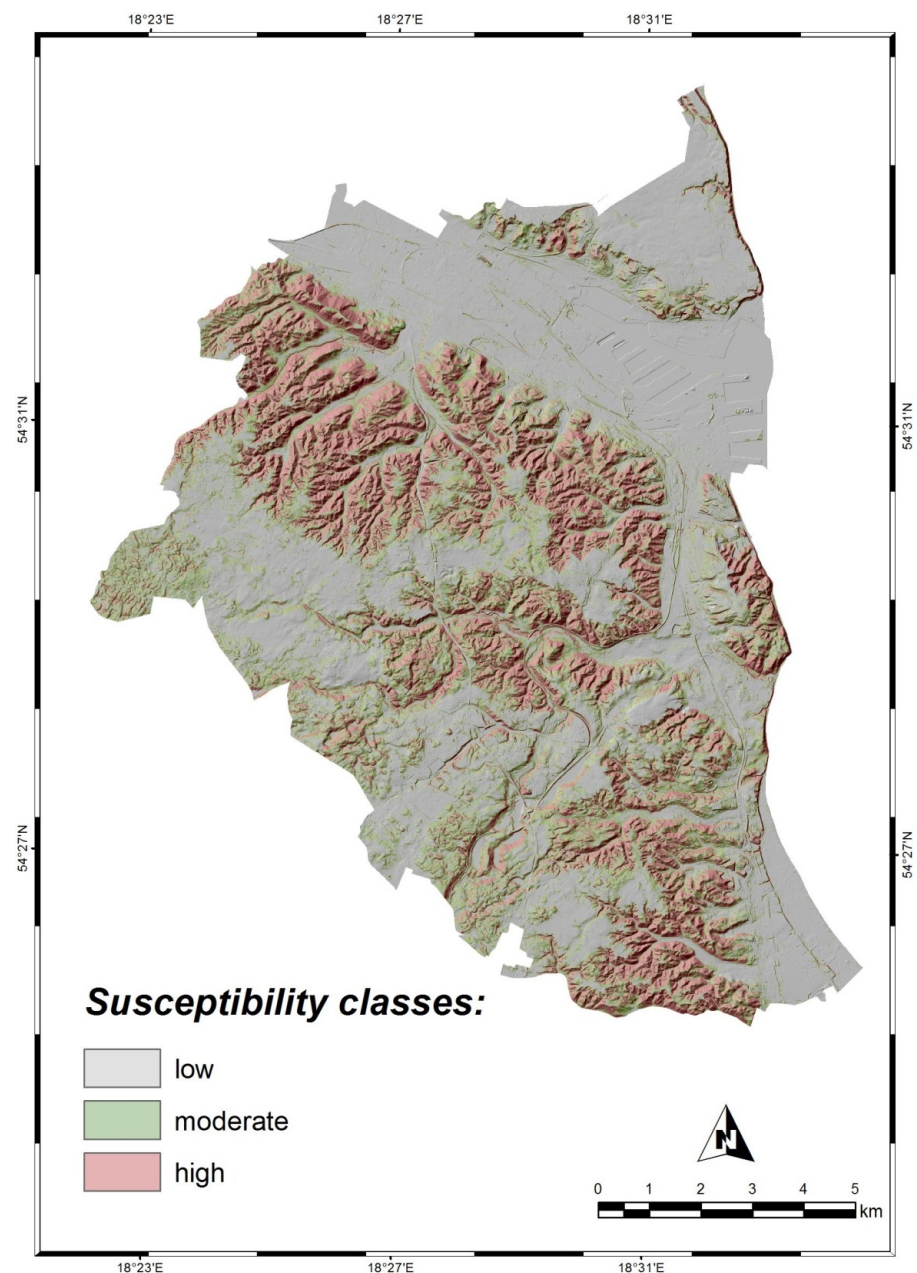
Figure 7. Landslide susceptibility map of Gdynia and Sopot developed using statistical landslide index (SLI).

The highest (>2) landslide susceptibility index values were determined for the LS index, slope angle, and relief energy. Most landslide areas occur at the angles of 10–29°. The value of the landslide susceptibility index increases with the greater angles both in Gdansk and Gdynia. Additionally, the interdependence between the increase in LSI index value and the intensities of slope failures is evident. Geological structure, especially the lithological diversity of strata, is an important triggering factor for mass wasting processes in Gdansk and Gdynia. The LSI index values show that landslides develop in loose (permeable) sediments (in Gdansk, for soils $\ln Wi = 0.46$, for sand and gravels $\ln Wi = 0.04$; in Gdynia, for soils 1.38) that occur above cohesive (impermeable/poorly permeable) ones (in Gdansk, for glacial till $\ln W_i = 0.06$; in Gdynia—for glacial till $\ln Wi = 0.17$). Hydrological and hydrogeological conditions are the next factors controlling mass wasting in Gdansk and Gdynia. The slopes in the vicinity (up to 50 m) of watercourses and reservoirs (in Gdansk, $\ln Wi = 0.84$, in Gdynia, $\ln Wi = 0.88$) are especially at risk. In Gdansk, the SLI reach

high values for the TWI interval of −0.6–2.6 (lnWi = 1.84). In Gdynia, the highest values of LSI (lnWi = 1.12) were observed for the TWI interval of 0–3, accounting for 43.33% of landslides [7]. This indicates the link between predominantly shallow mass movements and soil moisture parameters in Gdansk and Gdynia. A shallow groundwater table is frequently associated with the surface of rupture and demonstrates its role in landslide susceptibility (in Gdansk, for the groundwater table interval of 1–2 m lnWi = 0.24; in Gdynia, for the groundwater table interval of 0.5–1 m lnWi = 0.88).
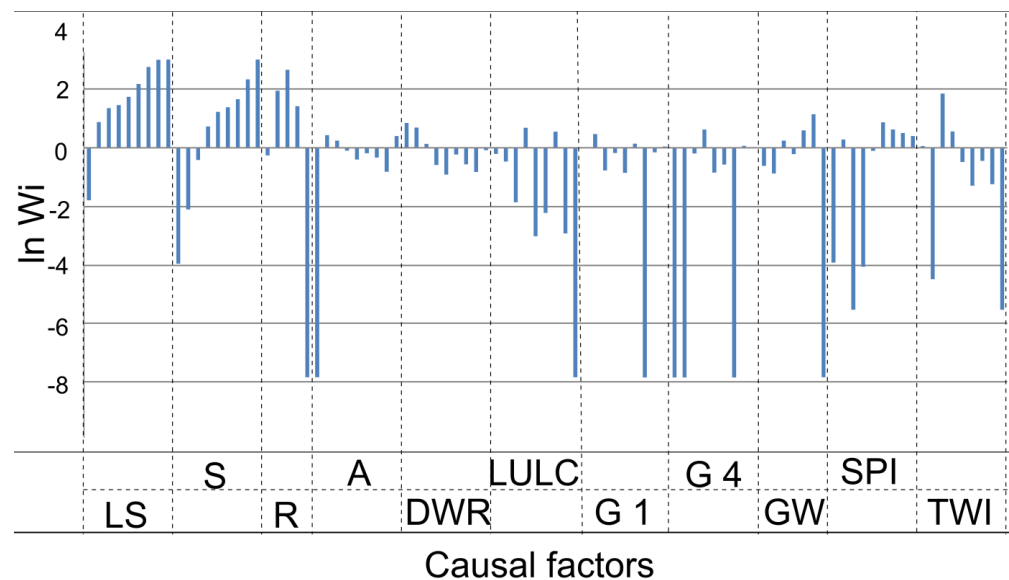

Figure 8. Importance of the conditioning factors for all landslides by the landslide susceptibility index (LSI) for entire landslide area in Gdansk.
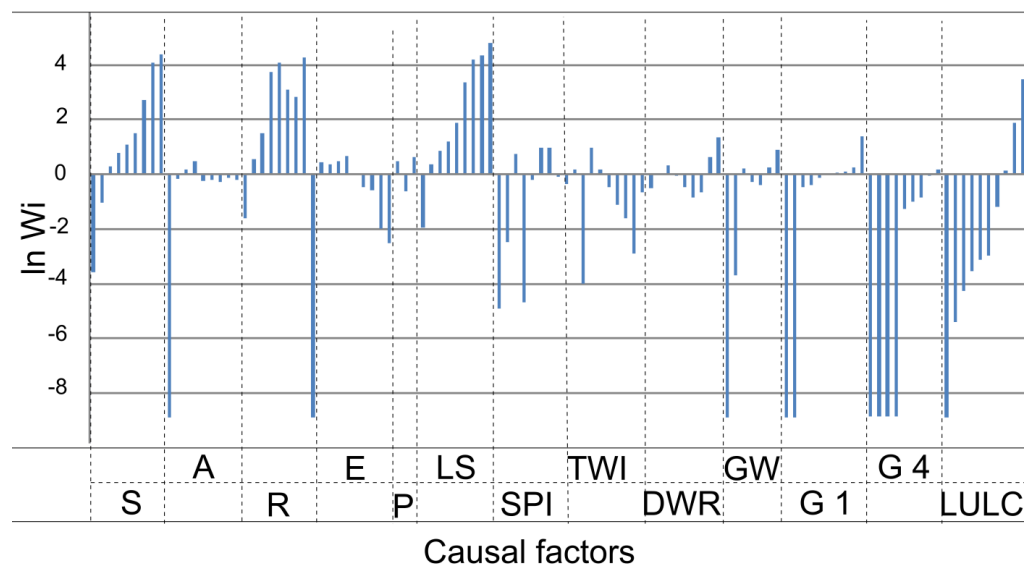

Figure 9. Importance of the conditioning factors for all landslides by the landslide susceptibility index (LSI) for entire landslide area in Gdynia.

6. Discussion

Susceptibility maps were made for both Gdansk [6] and Gdynia [7,32] on the basis of a detailed landslide inventory [3,4,32,36]. For the last 16 years, inventories of landslides in Poland have been compiled under a nationwide project, the Landslide Counteracting System [65,69]. However, these inventories are very expensive and are not yet produced for

the entire area of Poland. It is therefore appropriate to consider to what extent landslide data from neighboring areas can be used for areas for which we do not have such information.

However, the landslide susceptibility map prepared for Gdynia and Sopot on the basis of data extrapolated from Gdansk can only be indicative. Repeated modelling of susceptibility for Gdynia and Sopot using different variants of eleven causal factors and extrapolated landslide susceptibility index values for Gdansk and validation showed that such a wide set of causal factors does not produce reliable results. After multiple iterations, limiting the analysis to the five selected factors (Figure 6) yielded the best results, as shown by the validation results with the landslides in Gdynia, documented in 2012. On the other hand, the complete inventory of landslides for Gdynia and the susceptibility assessment performed on this basis using the landslide susceptibility index clearly show that sometimes different classes of causal factors are of different importance in the formation of landslides in Gdansk and Gdynia (Table 3). Particular attention should be paid to classes where this significance is quite different. The northern slope aspect is susceptible to landslides in Gdansk (lnWi = 0.43), while in Gdynia it is an unfavorable factor (lnWi = −0.17). On the other hand, the eastern slope aspect in Gdynia is the most favorable factor (lnWi = 0.49), whereas in Gdansk it is an unfavorable factor (lnWi = −0.10). In the upland area of Gdansk, landslides occur mainly along the entire slope lengths or at their bottom parts, with north, north-west and north-east aspects. The north-facing slopes retain snow longer than the south-oriented slopes. They also have an increased infiltration of precipitation and snowmelt. In the Tri-City, valley slopes with a northern orientation show higher relative humidity values compared to the southern ones, sometimes up to 3% [70]. Increased infiltration of the northern slopes may affect soil moisture parameters and the liquefaction of fine-grained and silty sediments. As a result, shallow mass movements may be activated. In the case of the slope aspect of Gdynia, eastern slopes (lnWi = 0.49) are the most predisposed to landslides, which should be associated with the orientation of coastline (Figure 1; Table 3). In the young morainic area of Gdynia, coastal abrasion is crucial for the reactivation of mass movement.

The landslide susceptibility index in Gdansk reaches higher values in forests (lnWi = 0.68; Table 3). The high landslide susceptibility of forested areas should be treated as a consequence, rather than a cause. Forests are a slope stabilizing factor as vegetation, through interception, retains some of the water soaked up by the earth, while capillary phenomena prevent the soil's saturation with water, on top of which deep roots contribute to soil drainage and lower pore pressure [71]. The higher landslide susceptibility of forested areas determined by the analysis is related to anthropogenic land use. Most of the Tri-City forests are located in areas with steep terrain and high relief energy (Figures 4 and 6). Centuries of human impact on the environment have caused the deforestation of the Żuławy Lowland and the Vistula Spit, while the hypsometrically diversified fringes of the upland have remained largely undeveloped.

In the case of the Tri-City area, cutting down forests on varied lithology slopes and in the areas susceptible to being washed away is certainly a landslide activating factor. In Gdynia, forested areas are not predisposed to landslides, (ln W = −0.13; Table 3). Additionally, the cutting down of a forest in Sopot Górny (Upper Sopot) in connection with the planned construction of a ski jump caused the occurrence of a new landslide. The landslide developed in the upper part of the slope with tills and multiple Miocene sandy-clayey xenoliths with lignite, and deeper situated fluvioglacial sands and gravels. Likewise, in Oliwa (Gdansk), the devastation of the forest activated mass wasting in the form of earth flow and earth creep on the slopes of Pachołek Hill.

The situation is similar for the other classes of causal factors (Table 3). However, factor slope does not show such a large variation. In addition, the slope factor is easy to count in most geoinformation programs such as ArcGIS, QGIS, and SAGA. For this reason, the slope factor can be most suitable for the development of susceptibility maps in young glacial areas, where there is no information on landslides.

Most landslides in the Tri-City occur in areas with steep slopes > 14° (Table 3). These results differ from those obtained in similar GIS analyses performed for the Carpathian

Mountains (Poland) where, for example, in the Lower Beskid (Beskid Niski) range the greatest susceptibility was observed on slopes of 9–14°, whereas greater gradients display a clear decrease in the lnWi index [22]. The neighboring area near Szymbark (Lower Beskid), in turn, displays the greatest susceptibility with angles of 5–7° and 18–20° [20]. Similar results were obtained by Wojciechowski near Nowy Sącz, where landslides occupy the largest areas on slopes of 7°–11° (2009) [72]. The reason may lie in a different geological structure, because young glacial areas contain cohesive tills. They form steep slopes, especially in cliffs, with some of them angled at >80°, while earth fall predominates in mass wasting processes. The high gradient of the Tri-City slopes with landslide occurrences can be traced back to a different role of the relief-forming processes which shaped the slopes. The processes of the last substage of the Vistulian Glaciation played a decisive role in shaping the major relief features [43]. Most slopes were formed by erosion over a relatively short period of time, from 10,000 to 12,000 years ago. In the case of the Carpathians, gentle slopes were formed on low-strength shale sediments. These sediments have poor resistance to degrading factors and are the most susceptible to landslides [73]. Furthermore, high-resolution LIDAR data was used in this analysis to calculate slope angles, which may also have influenced the results. More methodologically correct detailed angle comparisons for slopes with landslide occurrences in various regions of Poland require the same kinds of source data. According to Burdziej and Kunz [74], the DEM acquisition method has a significant influence on DEM's accuracy in high resolutions (from 1 to 25 m), with the most serious errors corresponding to the forms with the greatest slope angles.

Not all the causal factors which affect mass wasting can be visualized as a parameter map; in the case of young glacial areas, the greatest difficulties are caused by crustal deformation associated with glacial thrusting (glaciotectonic deformation; Figure 2b,c) and the presence of perched groundwater, which are some of the major factors in landslide occurrence. Quaternary deposits are also a problem as the available digital geological data depicts only the general regularities of Pleistocene and Holocene formations. These sediments are of a highly variable character in terms of type and method of deposition, even over a distance of several meters. Such a detailed digital visualization of geological data is currently not possible for large areas of cities.

7. Conclusions

The digital elevation model, originating from airborne laser scanning (LIDAR data) proved very useful in landslide susceptibility studies. Based on the DEM, primary and secondary topographic attributes can be calculated. The TWI and the SPI are well suited for modelling landslides in which earthflow is the predominating mass movement. These types of landslides often occur in unconsolidated Quaternary formations (sands, gravels, silts).

The performed landslide susceptibility analysis for the Tri-City demonstrated relationships between landslides and causal factors: the LS index, slope angle, slope aspect, TWI, SPI, lithology, distance from watercourses and reservoirs, the groundwater table level, and land use. Potential landslide areas have been indicated, particularly in the Tri-City Landscape Park, the fringes of the morainic upland, and a number of erosional-denudational valleys of the Kashubian Lakeland morainic upland. The SLI analysis for Gdansk and Gdynia has shown increased landslide susceptibility on slopes with a 10–29° gradient, developed in sediments with lithological diversity in their stratigraphic profile, characterized by the presence of interbedded silty sands, silts, and clays. The co-occurrence of loose sediments above cohesive ones is conducive to the infiltration of precipitation and to the initiation of slip surfaces. A close proximity of surface water is significant due to the major role played in mass wasting by fluvial erosion, as well as the drainage function.

The new aspect presented in this article is the comparison of two susceptibility maps created using the same method for neighboring urbanized areas. The difficulty of extrapolating landslide data for neighboring urban areas was indicated. In the case of Gdansk, which had been covered by comprehensive geological mapping, the best modelling results were obtained when a large number of causal factors were taken into account. In Gdynia

and Sopot, in turn, for which the SLI value was extrapolated from Gdansk, the best results were obtained when only five selected causal factors were included. This can be related to a different role of some causal factor classes in the occurrence of landslides in these areas, as well as the major significance of marine abrasion in landslide occurrence on the cliffs of Oksywie and Redłowo Hillocks.

The comparison of the two landslide susceptibility maps of Gdansk [6] and Gdynia [7] made using the SLI method also confirms the different importance of causal factors for neighboring urban areas.

Data Availability Statement: Not applicable.

Conflicts of Interest: The author has no financial or proprietary interest in any material discussed in this article.

References

1. Jurys, L.; Uścinowicz, G.; Małka, A.; Szarafin, T.; Zaleszkiewicz, L.; Pączek, U.; Frydel, J.; Kawęcka, J.; Prześdziecki, P. Identyfikacja zagrożen wywołanych ruchami masowymi w przestrzeni zurbanizowanej na przykładzie map osuwisk Gdanska i Gdyni. *Gór. Odkryw.* **2014**, *2–3*, 116–126, (In Polish with English summary).

2. Frydel, J.; Mil, L.; Jurys, L.; Maszloch, E.; Tobojko, L.; Karwacki, K. *Protokół Obserwacji z Monitoringu 3 Osuwisk Zlokalizowanych w Gdansku Przy ul. Malczewskiego, ul. Oginskiego oraz ul. Stromej, PGI NRI*; National Geological Archives: Gdansk, Poland, 2021.

3. Jurys, L.; Frydel, J.; Kaulbarsz, D.; Małka, A.; Pączek, U.; Szarafin, T.; Woźniak, T.; Zaleszkiewicz, L. Rejestr Osuwisk i Terenów Zagrożonych Ruchami Masowymi Ziemi w Skali 1:10 000 dla Terenu Miasta Gdanska. Register of Landslides and Areas Prone to Mass Movements with a Scale of 1: 10,000 for the City of Gdansk. 2011. Available online: https://download.cloudgdansk.pl/gdansk-pl/d/20121143147/rejestr-osuwisk-i-terenow-zagrozonych-ruchami-masowymi-ziemi-dla-terenu-miasta-gdanska.pdf (accessed on 23 August 2022). (In Polish)

4. Jurys, L.; Małka, A.; Pączek, U.; Szarafin, T. Rejestr Osuwisk i Terenów Zagrożonych Ruchami Masowymi Ziemi w Skali 1:10,000 dla Terenu Miasta Gdyni. Register of Landslides and Areas Prone to Mass Movements with a Scale of 1: 10,000 for the City of Gdynia. 2012. Available online: http://geoportal.pgi.gov.pl/ (accessed on 23 August 2022). (In Polish)

5. Szarafin, T.; Małka, A.; Jurys, L.; Frydel, J. Map of Landslides and Risk Areas for the City of Gdynia, in Scale 1:10,000. PGI–NRI. 2015. Available online: http://osuwiska.pgi.gov.pl/ (accessed on 23 August 2022). (In Polish)

6. Małka, A. Modelowanie podatności osuwiskowej z zastosowaniem metody indeksowej i wysokorozdzielczych danych z lotniczego skaningu laserowego (LIDAR) na obszarze Gdanska. *Przegląd Geol.* **2015**, *63*, 301–311, (In Polish with English summary)

7. Małka, A. Landslide Susceptibility Mapping in Urbanised Areas using Geographic Information System–Based Statistical Models: A Case Study of Gdynia, Poland. *Nat. Hazards* **2021**, *107*, 639–674. [CrossRef]

8. Sultana, N.; Tan, S. Landslide mitigation strategies in southeast Bangladesh: Lessons learned from the institutional responses. *Int. J. Disaster Risk Reduct.* **2021**, *62*, 102402. [CrossRef]

9. Stefanidis, S.; Chatzichristaki, C.; Stefanidis, P. An ArcGIS toolbox for estimation and mapping soil erosion. *J. Environ. Prot. Ecol.* **2021**, *22*, 689–696.

10. Naghibi, S.A.; Hashemi, H.; Pradhan, B. APG: A novel python-based ArcGIS toolbox to generate absence-datasets for geospatial studies. *Geosci. Front.* **2021**, *12*, 101232. [CrossRef]

11. Fell, R.; Corominas, J.; Bonnard, C.; Cascini, L.; Leroi, E.; Savage, W.Z. Guidelines for landslide susceptibility, hazard and risk zoning for land use planning. *Eng. Geol.* **2008**, *102*, 85–98. [CrossRef]

12. Fell, R.; Corominas, J.; Bonnard, C.; Cascini, L.; Leroi, E.; Savage, W.Z. Commentary. Guidelines for landslide susceptibility, hazard and risk zoning for land use planning. *Eng. Geol.* **2008**, *102*, 99–111. [CrossRef]

13. Corominas, J.; van Westen, C.; Frattini, P.; Cascini, L.; Malet, J.P.; Fotopoulou, S.; Catani, F.; van den Eeckhaut, M.; Mavrouli, O.; Agliardi, F.; et al. Recommendations for the quantitative analysis of landslide risk. *Bull. Eng. Geol. Environ.* **2014**, *73*, 209–263. [CrossRef]

14. Van Westen, C.J.; Ranwers, N.; Terlin, M.T.J.; Soeters, R. Prediction of the occurrence of slope instability phenomena through GIS-based hazard zonation. *Geol. Rundsch.* **1997**, *86*, 404–414. [CrossRef]

15. Van Westen, C.J.; Seijmonsbergen, A.C.; Montavani, F. Comparing Landslide Hazard Maps. *Nat. Hazards* **1999**, *20*, 137–158. [CrossRef]

16. Huabin, W.; Gangjun, L.; Weiya, X.; Gonghui, W. GIS-based landslide hazard assessment: An overview. *Prog. Phys. Geogr.* **2005**, *29*, 548–567. [CrossRef]

17. Sarkar, S.; Kanungo, D.P.; Patra, A.K.; Kumar, P. GIS Based Spatial Data analysis for Landslide Susceptibility Mapping. *J. Mt. Sci.* **2008**, *5*, 52–62. [CrossRef]

18. Pourghasemi, H.R.; Moradi, H.R.; Fatemi Aghda, S.M. Landslide susceptibility mapping by binary logistic regression, analytical hierarchy process, and statistical index models and assessment of their performances. *Nat. Hazards* **2013**, *69*, 749–779. [CrossRef]

19. Reichenbach, P.; Rossi, M.; Malamud, B.; Mihir, M.; Guzzetti, F. A review of statistically-based landslide susceptibility models. *Earth-Sci. Rev.* **2018**, *180*, 60–91. [CrossRef]

20. Mrozek, T.; Poli, S.; Sterlacchini, S.; Zabuski, L. Landslide susceptibility assessment. A case study from the Beskid Niski Mts., Carpathians, Poland. *Polish Geol. Inst. Sp. Pap.* **2004**, *15*, 13–18.

21. Kaminski, M. Mapa podatności osuwiskowej w skali regionalnej—Przykład z Doliny Sanu na Pogórzu Dynowskim. *Biul. Panstwowego Inst. Geol.* **2012**, *452*, 109–118.

22. Długosz, M. *Podatność Stoków na Osuwanie w Polskich Karpatach Fliszowych*; Pr. Geogr. 230; IGiPZ PAN: Warszawa, Poland, 2011; pp. 1–112.

23. Mrozek, T. Zagrożenie i ryzyko osuwiskowe w rejonie Szymbarku (Beskid Niski). *Pr. Panstwowego Inst. Geol.* **2013**, *199*, 5–40. (In Polish)

24. Mrozek, T.; Laskowicz, I. Landslide risk reduction in Poland: From landslide inventory to improved mitigation and landuse practice in endangered areas. In *Landslide Science for a Safer Geoenvironment*; Methods of Landslide Studies; Sassa, K., Canuti, P., Yin, Y., Eds.; Springer: Cham, Switzerland, 2014; Volume 2, pp. 765–771.

25. European Commission. *Thematic Strategy for Soil Protection*; COM(2006)231 final; Commission of the 17 European Communities: Brussels, Belgium, 2006.

26. European Commission. *A Community Approach on the Prevention of Natural and Man-Made Disasters*; COM(2009) 82 final; European Commission: Brussels, Belgium, 2009.

27. European Commission. *New EU Forest Strategy for 2030*; COM(2021)572 final; Commission of the 17 European Communities: Brussels, Belgium, 2021.

28. Yalcin, A. GIS-based landslide susceptibility mapping using analytical hierarchy process and bivariate statistics in Ardesen (Turkey): Comparisons of results and confirmations. *Catena* **2008**, *72*, 1–12. [CrossRef]

29. Magliulo, P.; Di Lisio, A.; Russo, F.; Zelando, A. Geomorphology and landslide susceptibility assessment using GIS and bivariate statistics: A case study in southern Italy. *Nat. Hazards* **2008**, *47*, 411–435. [CrossRef]

30. Wang, Q.; Li, W.; Wu, Y.; Pei, Y.; Xie, P. Application of statistical index and index of entropy methods to landslide susceptibility assessment in Gongliu (Xinjiang, China). *Environ. Earth Sci.* **2016**, *75*, 599. [CrossRef]

31. Liu, J.; Duan, Z. Quantitative assessment of landslide susceptibility comparing statistical index, index of entropy, and weights of evidence in the Shangnan Area, China. *Entropy* **2018**, *20*, 868. [CrossRef] [PubMed]

32. Małka, A. Podatność i ryzyko osuwiskowe w obszarach rzeźby młodoglacjalnej, przeobrażonej antropogenicznie, na terenie Gdyni (Landslide Susceptibility and Risk in the Anthropogenically Transformed Postglacial Areas in Gdynia). Ph.D. Thesis, PIG-PIB, Warszawa, Poland, 2018. [CrossRef]

33. De Smith, M.J.; Goodchild, M.F.; Longley, P.A. *Geospatial Analysis: A Comprehensive Guide to Principles, Techniques and Software Tools*, 6th ed.; Amazon Italia Logistica S.r.l.: Turin, Italy, 2018.

34. Wang, Q.; Wang, Y.; Niu, R.; Peng, L. Integration of Information Theory, K-Means Cluster Analysis and the Logistic Regression Model for Landslide Susceptibility Mapping in the Three Gorges Area, China. *Remote Sens.* **2017**, *9*, 938. [CrossRef]

35. Fang, Z.; Wang, Y.; Duan, G.; Peng, L. Landslide Susceptbiity Mapping Using Rotation Forest Ensemble Technique with Different Decision Trees in the Three Gorges Reservoir Area, China. *Remote Sens.* **2021**, *13*, 238. [CrossRef]

36. Szpakowski, W.; Szydłowski, M. Probable rainfall in Gdansk in view of climate change. *Acta Sci. Pol. Formatio Circumiectus* **2018**, *18*, 175–183. [CrossRef]

37. Miętus, M.; Filipiak, J. The patterns of thermal conditions in the area of the southern coast of the Gdansk (N Poland). In Proceedings of the Fifth International Conference on Urban Climate, Łódź, Poland, 1–5 September 2003.

38. Schrötter, F.L. *Karte von Ost-Preussen nebst Preussisch Litthauen und West-Preussen nebst dem Netzdistrict aufgenommen unter Leitung des Königl. Preuss. Staats Ministers Frey Herrn von Schroetteer in den Jahren von 1796 bis 1802*; Berlin State Library: Berlin, Germany, 1806.

39. Falckenstein. *Topographische Karte, Maßstab 1:25 000, Blatt Danzig*; Berlin State Library: Berlin, Germany, 1837.

40. Lattre. *Topographische Karte, Maßstab 1:25 000, Blatt Oliva*; Berlin State Library: Berlin, Germany, 1862.

41. Kwoczynska, B. Analysis of land use changes in the Tri-City metropolitan area based on the multi-temporal classification of LANDSAT and RAPIDEYE imagery. *GLL Geomat. Landmanagement Landsc.* **2021**, *2*, 101–119. [CrossRef]

42. Mojski, J.E. *Ziemie Polskie w Czwartorzędzie*; Zarys morfogenezy; PGI–NRI: Warszawa, Poland, 2005. (In Polish)

43. Woźniak, P.P. Development of morphology and sedimentary profiles on Kashubian Coastline during the Vistulian glaciation—An outline of main problems. In *Evolution of Sedimentary Environments in Pobrzeże Kaszubskie Region*; Sokołowski, R.J., Ed.; Uniwersytet Gdanski: Gdynia, Poland, 2014; pp. 17–26. (In Polish)

44. Kondracki, J. *Geografia Regionalna Polski*; PWN: Warszawa, Poland, 1998.
45. Sonntag, P. *Geologischer Führer Durch Die Danziger Gegend*; Verlag und Druck von A. W. Kafemann G.m.b.H.: Danzig, 1910.
46. Uścinowicz, S. Relative sea level changes, glacio-isostatic rebound and shoreline displacement in the southern Baltic. *Pol. Geol. Inst. Spec. Pap.* **2003**, *10*, 5–79.
47. Gałka, M.; Holger-Knorr, K.; Miotk-Szpiganowicz, G.; Moskalewicz, D.; Sz, U.; Witak, M.; Woźniak, P. Environmental setting of the stone age settlement complex at the Rzucewo site. In *Stone Age Settlement Complex in Rzucewo, Site 1, Puck Commune*; Król, D., Ed.; Muzeum Archeologiczne w Gdansku: Gdansk, Poland, 2018; pp. 14–39. (In Polish)
48. Małka, A. Mass movements in the area of Gdynia documented on old maps and in archival materials. *Przegląd Geol.* **2019**, *67*, 308–319. Available online: https://link.springer.com/article/10.1007/s11069-021-04599-8 (accessed on 8 January 2020). (In Polish with English summary)
49. Zawadzka-Kahlau, E. *Tendencje Rozwojowe Polskich Brzegów Południowego Bałtyku*; GTN: Gdansk, Poland, 1999.
50. Wyrzkowski, T. *Map of Recent Vertical Movement of the Earth Crust on the Territory of Poland 1:2500000*; Inst. Geod. i Kart.: Warszawa, Poland, 1985.
51. Pikies, R.; Zaleszkiewicz, L. *Szczegółowa Mapa Geologiczna Polski w skali 1:50 000, Ark. Gdynia (55)—Reambulacja*; PIG–PIB: Warszawa, Poland, 2013.
52. Mojski, J.E. *Szczegółowa Mapa Geologiczna Polski 1:50 000, Ark. Gdansk (27)*; Wyd Geolog: Warszawa, Poland, 1977.
53. Mojski, J.E. *Szczegółowa Mapa Geologiczna Polski 1:50 000, Ark. Gdynia (16)*; Wyd Geolog: Warszawa, Poland, 1978.
54. Frankowski, Z.; Zachowicz, J.; Gałkowski, P.; Jaros, M.; Majer, K.; Pasieczna, A.; Lis, J.; Mil, L.; Jurys, L.; Lidzbarski, M.; et al. Baza Danych Geologiczno-Inżynierskich Wraz z Opracowaniem Atlasu Geologiczno-Inżynierskiego Aglomeracji Trójmiejskiej Gdansk—Sopot—Gdynia. Geological and Engineering Atlas of the Tri-City of Gdansk-Sopot-Gdynia Urban Area. PGI NRI. National Geological Archives. Warszawa. 2007. Available online: http://geoportal.pgi.gov.pl/atlasy_gi/atlasy/trojmiasto (accessed on 8 January 2020). (In Polish)
55. Lohani, B.; Ghosh, S. Airborne LiDAR technology: A review of data collection and processing systems. *Proc. Natl. Acad. Sci. India Sect. A* **2017**, *87*, 567–579. [CrossRef]
56. Urban Atlas–PL006L–Gdansk. European Environment Agency (EEA). Copenhagen. 2010. Available online: http://www.eea.europa.eu/data-and-maps/data/urban-atlas (accessed on 23 August 2022).
57. Wu, W.; Sidle, R.C. A distributed slope stability model for steep forested basins. *Water Resour. Res.* **1995**, *31*, 2097–2110. [CrossRef]
58. Van Westen, C.J.; Castellanos, E.; Kuriakose, S.L. Spatial data for landslide susceptibility, hazard, and vulnerability assessment: An overview. *Eng. Geol.* **2008**, *102*, 112–131. [CrossRef]
59. Wilson, J.P.; Gallant, J.C. *Terrain Analysis: Principles and Applications*; Wiley: New York, NY, USA, 2000.
60. Moore, I.D.; Grayson, R.B.; Ladson, A.R. Digital terrain modelling: A review of hydrical, geomorphological, and biological applications. *Hydrol. Process.* **1991**, *5*, 3–30. [CrossRef]
61. Sharma, A.K.; Gardner, T.; Begbie, D. *Approaches to Water Sensitive Urban Design*; Woodhead Publishing: Cambridge, UK, 2019. [CrossRef]
62. Dai, F.C.; Lee, C.F.; Ngai, Y.Y. Landslide risk assessment and management: An overview. *Eng. Geol.* **2002**, *64*, 65–87. [CrossRef]
63. Cordy, G.E. NBMG Open File Report 87–5. Geology and Earthquake Hazards. Reno NE Quadrangle. University of Nevada Reno. Nevada Bureau of Mines and Geology. 1987. Available online: https://citeseerx.ist.psu.edu/viewdoc/download?doi=10.1.1.214.4577&rep=rep1&type=pdf (accessed on 23 August 2022).
64. Goetz, J.N.; Guthrie, R.H.; Brenning, A. Integrating physical and empirical landslide susceptibility models using generalized additive models. *Geomorphology* **2011**, *129*, 376–386. [CrossRef]
65. Grabowski, D.; Marciniec, P.; Mrozek, T.; Nescieruk, P.; Rączkowski, W.; Wojcik, A.; Zimnal, Z. *Instrukcja Opracowania Mapy Osuwisk i Terenów Zagrożonych Ruchami Masowymi w Skali 1:10,000*; PGI NRI: Warszawa, Poland, 2008. (In Polish)
66. Jenks, G.F. The Data Model Concept in Statistical Mapping. *Int. Yearb. Cartogr.* **1967**, *7*, 186–190.
67. Veerappan, R.; Negi, A.; Siddan, A. Landslide susceptibility mapping and comparison using frequency ratio and analytical hierarchy process in part of NH-58, Uttarakhand, India. In *Advancing Culture of Living with Landslides*; Mikos, M., Tiwari, B., Yin, Y., Sassa, K., Eds.; Springer: Cham, Switzerland, 2017; Volume 2. [CrossRef]
68. Arabameri, A.; Saha, S.; Roy, J.; Chen, W.; Blaschke, T.; Tien Bui, D. Landslide Susceptibility Evaluation and Management Using Different Machine Learning Methods in The Gallicash River Watershed, Iran. *Remote Sens.* **2020**, *12*, 475. [CrossRef]
69. Marciniec, P.; Zimnal, Z.; Wojciechowski, T.; Perski, Z.; Rączkowski, W.; Laskowicz, I.; Nieścieruk, P.; Grabowski, D.; Kułak, M.; Wójcik, A. Osuwiska w Polsce—Od rejestracji do prognozy, czyli 13 lat projektu SOPO. Landslides in Poland: From registration to forecast, 13 years of the LCS project. *Prz. Geol.* **2019**, *67*, 291–297. (In Polish)
70. Szukalski, J. *Środowisko Geograficzne Trójmiasta (Gdansk–Sopot–Gdynia)*; UG. Skrypty Uczelniane: Gdansk, Poland, 1974.
71. Parriaux, A.; Bonnard, C.; Tacher, L. *Rutschungen: Hydrogeologie und Sanierungsmethoden durch Drainage. Leitfaden*; BUWAL: Bern, Switzerland, 2010.
72. Wojciechowski, T. Geologiczna analiza osuwisk z wykorzystaniem satelitarnej interferometrii radarowej na przykładzie rejonu Nowego Sącza. Ph.D. Thesis, Biblioteka Wydz, Nauk o Ziemi UŚ, Sosnowiec, Poland, 2009.

73. Bober, L. Regiony osuwiskowe w polskich Karpatach Fliszowych i ich związek z budową geologiczną regionu. *Biul. Inst. Geol.* **1984**, *340*, 115–158.

74. Burdziej, J.; Kunz, M. Estimation of resolution influence and methods of acquiring high-altitude data on the accuracy of numeric terrain models and models of slopes and aspects. *Arch. Fotogram. Kartogr. i Teledetekcji* **2006**, *16*, 111–123, (In Polish with English summary)